Neuronal Dynamics: From Hodgkin-Huxley to FitzHugh-Nagumo Model

Neil Gandhi: A09259792
Joshua Chu: A09359806
Adam Li: A09377908
Sophie Man: A09375793
Yifan Wu: A097421136

Neuronal Dynamics

Purpose of Neuronal Dynamic Modeling

Neurons are regulated on a cellular level by the biophysics of neuronal firing as well as on the molecular level by gene regulation. In addition, a network of neurons can interact with each other to produce nonlinear dynamics which relate to sensory, motor, and behavioral changes. Neurons are unique in their ability to transmit electrical signals over long distances, resulting in complex neural circuits, cortical structure, and the central nervous system (CNS). By analyzing the system, we can infer macroscopic behavior of the organism with applications toward medicine and technology.

Modeling neuronal dynamics has significant medical application. The mechanism behind neurological disorders, such as Parkinson's disease, autism, and epilepsy, are not well known but modeling neuronal systems can give insight into the neurodegeneration caused by these diseases and possibly ways to cure them.

In addition, modeling neuronal behavior has significant application in the computer industry, specifically neuromorphic engineering, which mimics the neuronal dynamics of the CNS into VLSI analog circuits. By modeling neuronal dynamics for processing purposes, low-power and high efficiency adaptable chip design can be achieved[1].

Background and Hodgkin-Huxley Model

Different mathematical models predict the behavior of neurons but one of the most well-regarded is the Hodgkin-Huxley (HH) model. This fourth-order system of nonlinear differential equations was proposed by Hodgkin and Huxley in 1952 as the culmination of experiments that they had performed on giant squid axons. The resulting system consisted of one variable describing the membrane potential and three voltage-gating variables characterizing the dynamics of different voltage-gated ion channels. Hodgkin and Huxley's model made extensive use of stochastic functions to describe the continuous random variables whose values were determined by experimental data. The remarkable ability of the model to predict the key biophysical properties of the action potential accurately helped Hodgkin and Huxley win the 1963 Nobel Prize in Physiology and Medicine at a time when voltage-gated ion channels had yet to be discovered[2].

The Hodgkin-Huxley (HH) model studies neurons as dynamic models with activation/inactivation of voltage-gated conductances. The HH Model is governed by a fourth-order system of nonlinear ordinary differential equations, with the 4 dimensions resulting from the membrane voltage and three voltage gating variables. Important

elements are the membrane capacitance, the ion-specific conductances and electrochemical gradients, and current sources (ion pumps)[2].

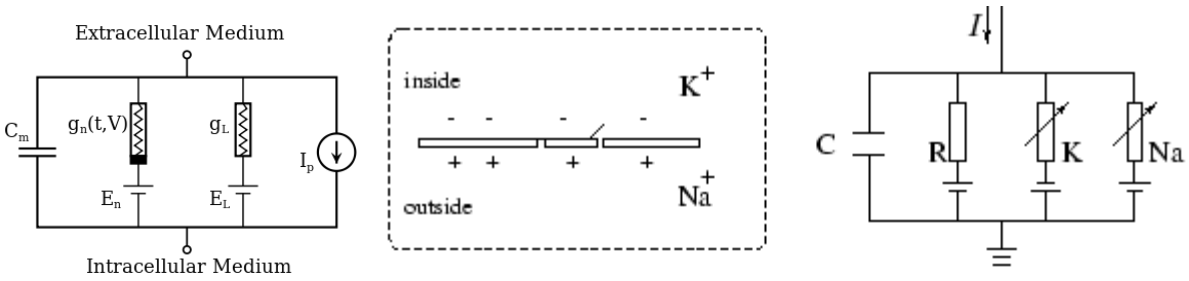

Figure 1: Cells contain a membrane potential, which when depolarized, creates an action potential. Here the membrane potential and the ion channels are modeled as circuit components (explained in further detail below).

The lipid bilayer separates the interior of the neuron from its surroundings. Due to the potential difference between the inside and outside of this cell, the lipid bilayer can be modeled as a membrane capacitance, with the current described by the changing electrochemical gradient, as given by

$$I_c = C_m \frac{dV_m}{dt};$$

The current through a given ion channel is

$$I_i = g_i(V_m - V_i)$$

where g_i is the variable conductance of that ion channel, V_m is the membrane potential, and V_i is the reversal potential of the specific channel. For the Hodgkin-Huxley model, these are sodium and potassium channels. In addition, the model takes into account leak channels, which are due primarily to chloride transport.

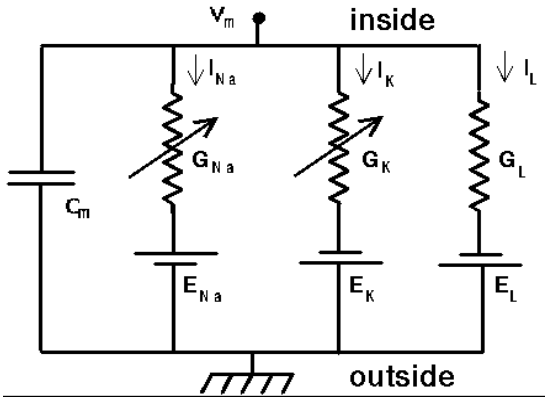

Figure 2: The Hodgkin-Huxley model with ion channels represented as conductances G_i, membrane potential as C_m, the membrane potential as V_m, and the current as I.

The differential equations that describe the biophysical characteristics (ionic currents) of action potentials in a neuron are the following.

$$C_m\, dV/dt = I_p - g_k n^4(V - E_k) - g_{Na} m^3 h(V - E_{Na}) - g_L(V - E_L) \quad (1)$$

$$dn/dt = \alpha_n(1 - n) - \beta_n n \quad (2)$$

$$dm/dt = \alpha_m(1 - m) - \beta_m m \quad (3)$$

$$dh/dt = \alpha_h(1 - h) - \beta_h h \quad (4)$$

Action potentials within neurons arise from time-variant and voltage-dependent changes in the conductance of neural membrane to specific ions. The ionic current is divided into components carried by sodium and potassium ions (I_{Na} and I_K) and a small leakage current (I_l) made up on chloride and other ions. Each component of the ionic current is determined by a driving force which may be measured as an electrical potential difference and a permeability coefficient which has the dimensions of conductance. The changes in permeability depend on membrane potential as do g_{Na} and g_K, suggesting that permeability changes arise from effect of electric field[2,3].

Aim

Our goal is to investigate neural dynamics by examining the phase portraits, bifurcations, nullclines, and vector field that result when certain parameters are adjusted, such as injected current. We then adapt the model in application toward a neurological disorder, namely epilepsy, in an attempt to gain understanding on how the disease differs from normal neuronal firing.

HH Model Simulation:

Giant squid axon data from Hodgkin and Huxley's original experiments were used, with these values shown in Table 1.[2]

Table 1
Parameter values in the H-H model.

C_M	1.0 μF/cm^2	V_{N_a}	115,0 mV	$\overline{g_{Na}}$	120.0 ms/cm^2	V_K	−12.0 mV
$\overline{g_K}$	36.0 ms/cm^2	V_l	10.599 mV	$\overline{g_l}$	0.3 ms/cm^2	T	6.3 °C

Table 1: Shows values for parameters in the Hodgkin-Huxley model for a giant squid.

Figure 3 shows the simulation results for the full 4D HH model. By solving the system of nonlinear ODEs using the Euler method, one can simulate the results of the Hodgkin-Huxley model. Beginning at 0ms, model is stimulated by a single current spike until 5 ms, then the current is set to 0 mA until 20ms. Staring at 20ms, 50 mA of current is continually applied until 100 ms. The figure depicts the membrane potentials well as the potassium and sodium conductances is shown in Figure 3. As illustrated in figure below, potassium channel opens first then follows the sodium channel. In addition, with the

continuous stimulation, the neuron does not have sufficient time to restore the electrochemical gradient. Therefore, subsequent depolarizations are reduced in magnitude.

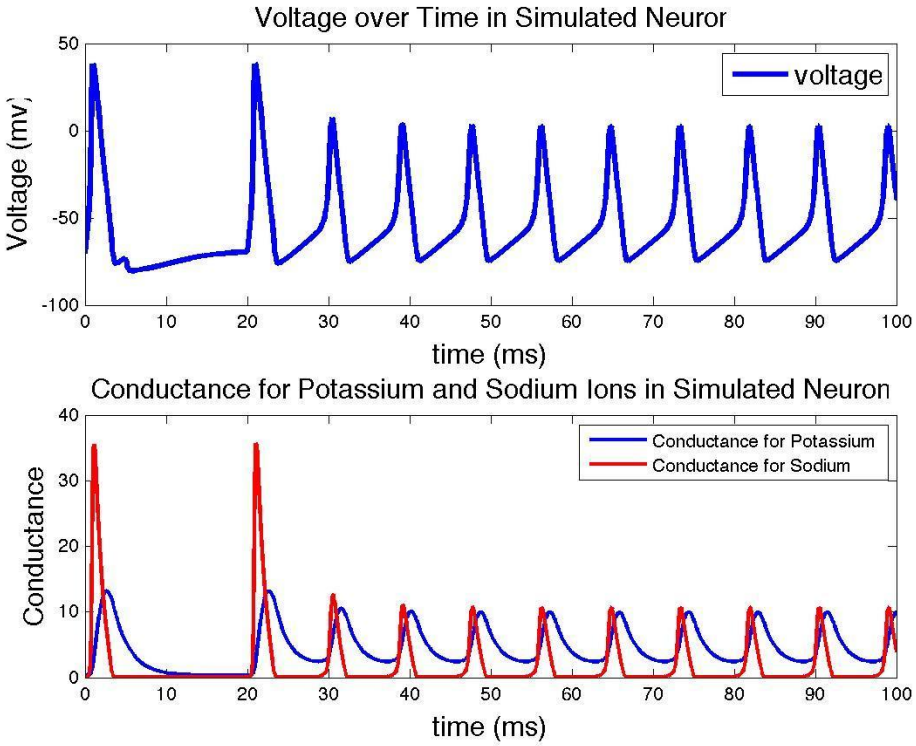

Figure 3. Simulation of HH model using giant squid neuron parameters. a. membrane potential change with stimulation. b. potassium and sodium conductances respond.

Figure 4 depicts the same Hodgkin-Huxley model but when the applied current is only 2 mA. This input current is below the threshold required for an action potential. Therefore, a small depolarization or perturbation in the positive direction is witnessed, but the membrane potential very quickly to resting potential. It is interesting to note that in this case, the resting potential acts as a stable fixed point. The oscillatory motion about the fixed point can be characterized as a damped oscillation, which occurs when the damping ratio is between 0 and 1^{st} in 2^{nd} order or higher systems.

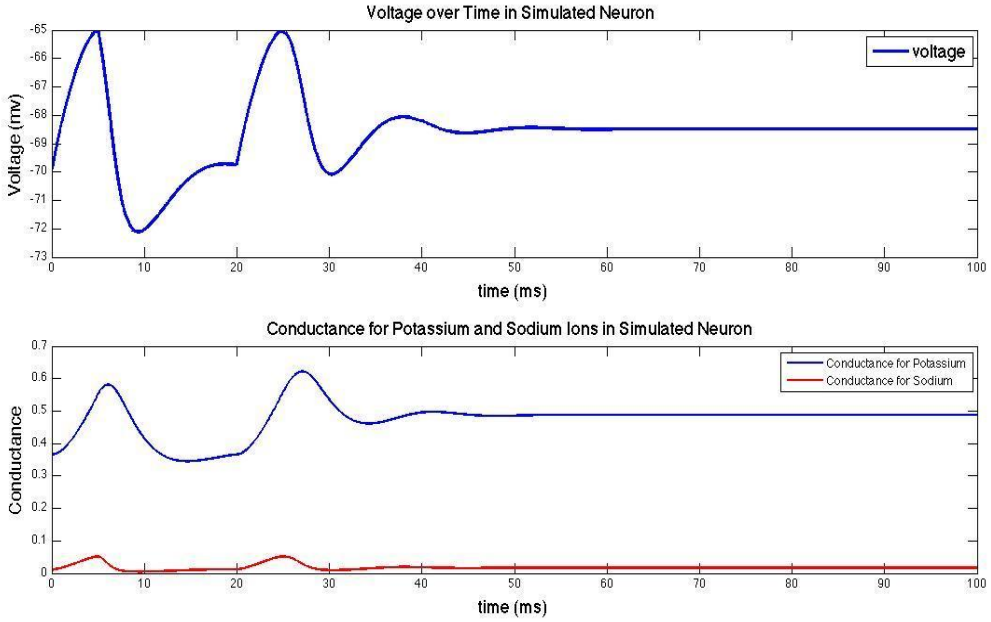

Figure 4. Membrane potential and ion channel conductances responding 2mA current stimulation. a. Membrane voltage. b. Potassium and sodium conductance.

Simplification of HH Model:

The full 4D HH model gives the most accurate representation of the time series for the membrane potential and voltage gating variables. However, it is difficult to understand graphically the qualitative dynamics of the entire system, particularly because only projections of the system can be visualized on a 2D or 3D plane. Fortunately the 4D HH model can be simplified without sacrificing the overall qualitative features of the original system. This would allow easier use of different analytical and graphical tools such as nullclines and bifurcation points, in order to analyze the qualitative states that the system can take.

The first level of simplification stems from empirical data gathered by Krinskii and Kokoz, who have shown that the potassium activation and sodium inactivation gates, 'n' and 'h', respectively, add up to 0.8, or n+h = 0.8 in equation (1). Moreover, since Na^+ gate kinetics are fast compared to the K^+ gate, we can assume that the Na^+ gating variable m is at its steady state level (m_∞), although this is still dependent on the membrane potential. Thus the final differential equations for the reduced HH model is a 2D system consisting of the membrane potential and potassium gate variable[3].

$$C_m \frac{dV}{dt} = -g_{Na} n^4 (V - V_K) - g_{Na} m_\infty^3(V)(0.8 - n)(V - V_{Na}) - g_L(V - V_L) + I_{appl}; \quad (5)$$

$$n_\omega(V) \frac{dn}{dt} = n_\infty(V) - n \quad (6)$$

A comparison between the reduced HH model and the original shows that the reduced model responds faster to the stimulus (Figure 5). This is to be expected since the Na^+

gating variable m was assumed to be at its steady state levels for all time. Although the two responses are not identical, the shapes of their waveforms are sufficiently similar to warrant the use of a 2D reduced system instead of the original 4D model.

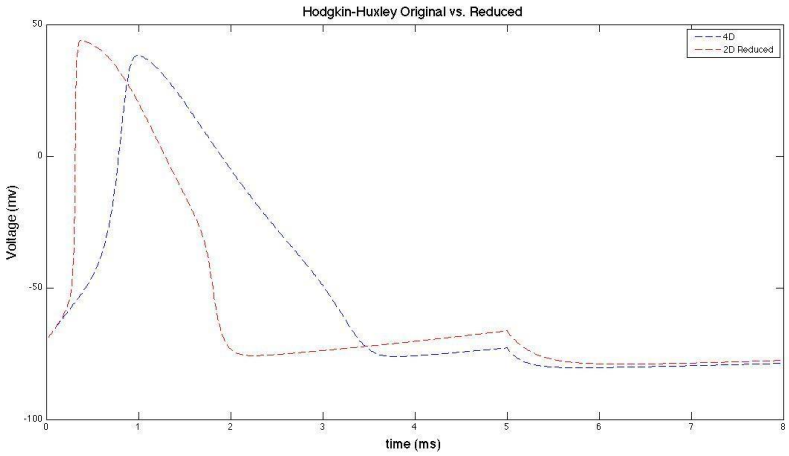

Figure 5. Membrane potential response for original HH model and reduced model for single current stimulation.

FitzHugh-Nagumo Model Characterization/Simulation:

The FitzHugh-Nagumo (FHN) model mimics the Hodgkin-Huxley model in a simplified manner by approximating the action potentials via cubic nullclines. The parameter $'\alpha'$ defines the shape of the cubic function and is the threshold for excitability, 'b' represents the excitability and 'c' is a parameter that can change the kinetics of the recovery variable. The equations below show the V-nullcline has the shape of a cubic function and the n-nullcline in equation (5) and (6) could be approximated by a straight line, suggesting that the polynomial model can be reduced[3,5]:

$$\frac{d\upsilon}{dt} = \upsilon(\upsilon - \alpha)(1 - \upsilon) - \omega + I \quad (7)$$

$$\frac{d\omega}{dt} = b(\upsilon - c\omega) \quad (8)$$

where $\upsilon$is the membrane potential, $\omega$is the ion gating variable and I is the stimulation current. For the giant squid axon, α=0.15, b=0.01 and c=0.02.

Fixed Points/Phase Portrait Analysis:

Using the FHN model, the v- and w-nullclines can be plotted, shown in Figure 6. The v-nullcline is the third order polynomial, and the w-nullcline is the straight line, with the vector field superimposed on the nullclines to show the trajectory of the phase portrait. Fixed points are determined as the intersection of the two nullclines. With initial conditions of a = 0.1, b= 0.01, and c = 0.1, three fixed points exist. Through visual inspection of the nullclines, one can see that the number of fixed points can be 1, 2, or 3, depending on the values of the parameters, which indicates the presence of

bifurcations. Graphically, a changes the shape of the υ-nullcline, and b and c change the slope of the ω-nullcline.

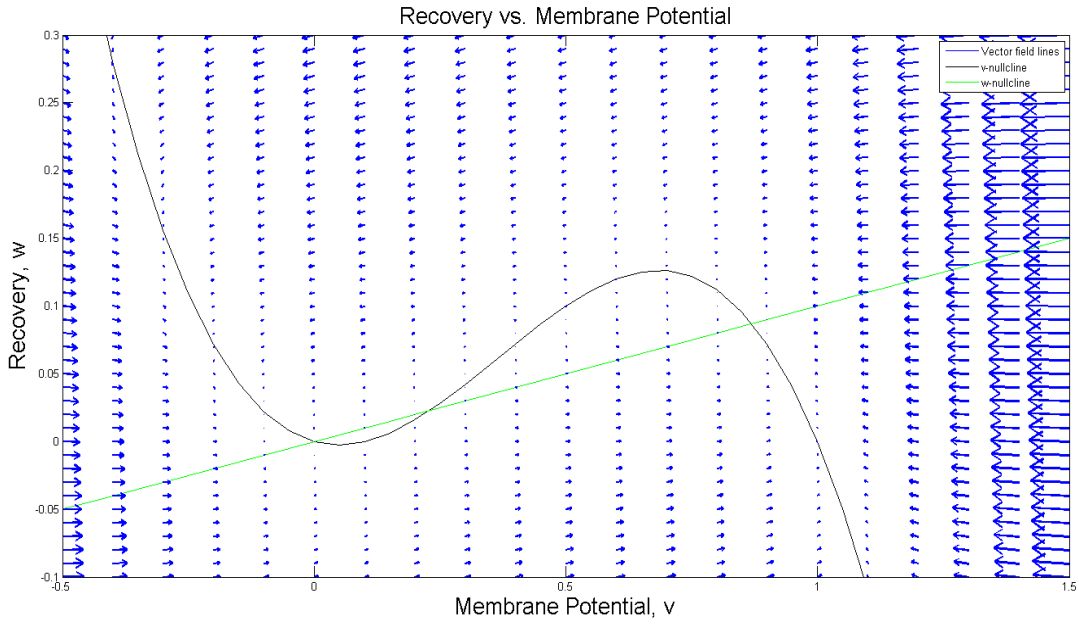

Figure 6: The nullclines are plotted along with the vector field. The three intersections correspond to three fixed points and the circular movement of the vector field indicates a limit cycle.

Bifurcations:

The Fitzhugh model as well as the Hodgkin-Huxley model exhibit the supercritical Hopf bifurcation. A Hopf bifurcation occurs when eigenvalues cross the imaginary axis as some some parameter μ varies. In this case, the parameter is the applied current. At the Hopf bifurcation, a stable spiral fixed point becomes an unstable fixed point and is surrounded by a closed orbit called the limit cycle. If the applied current is lower the critical value, μ_c, the system oscillates a little, then dampens to the original resting potential. This is represented by a stable spiral fixed point. When the applied current is increased greater than μ_c, sustained spiking occurs, which is described by the convergence of the unstable spiral to the limit cycle.

In Figure 7a,b, the simulations show a bifurcation occurring. Specifically, this shows a limit cycle disappearing on the phase portrait as the parameter a changes, where *a* is a parameter that affects the kinetic gating variables of the ion channels. In Figure 4a-b, we see the dynamics of the action potential changing in not only the phase diagram, but also the actual firing behavior. Increasing *a* from its initial value of 0.1 makes it more difficult for the external stimulus to produce an excitation until no activation is produced. We can test this experimentally by changing the ion concentrations within the cell,

therefore changing the threshold for excitability, and run trials at different points to validate this model.

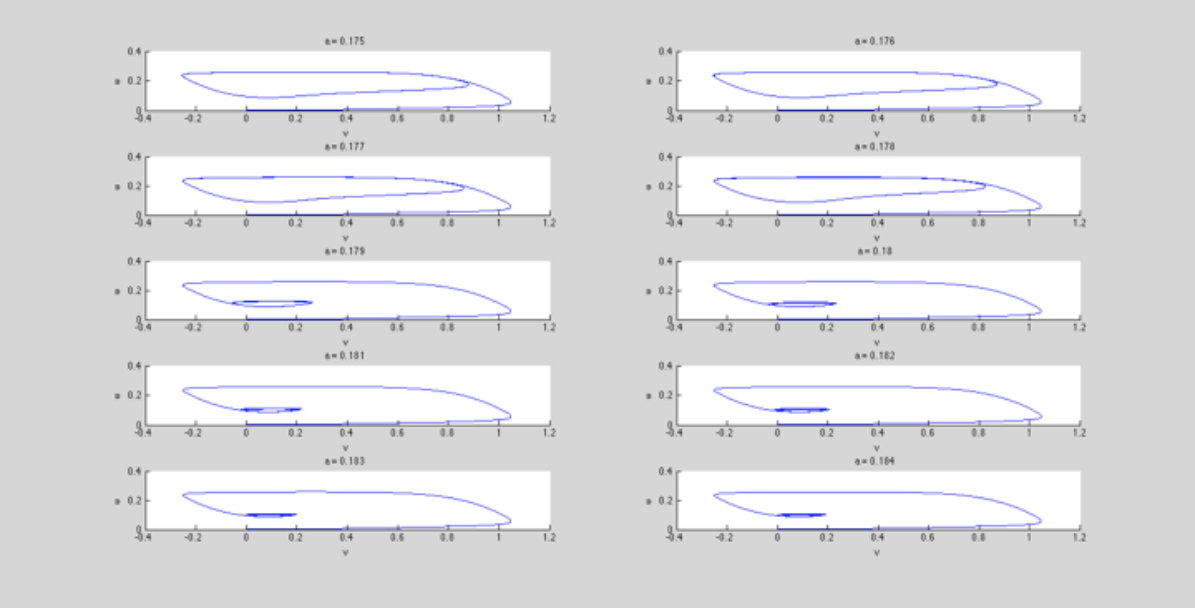

Figure 7a: These are phase portraits of ω vs υ. A bifurcation occurs as well as seen when the limit cycle becomes a stable spiral fixed point.

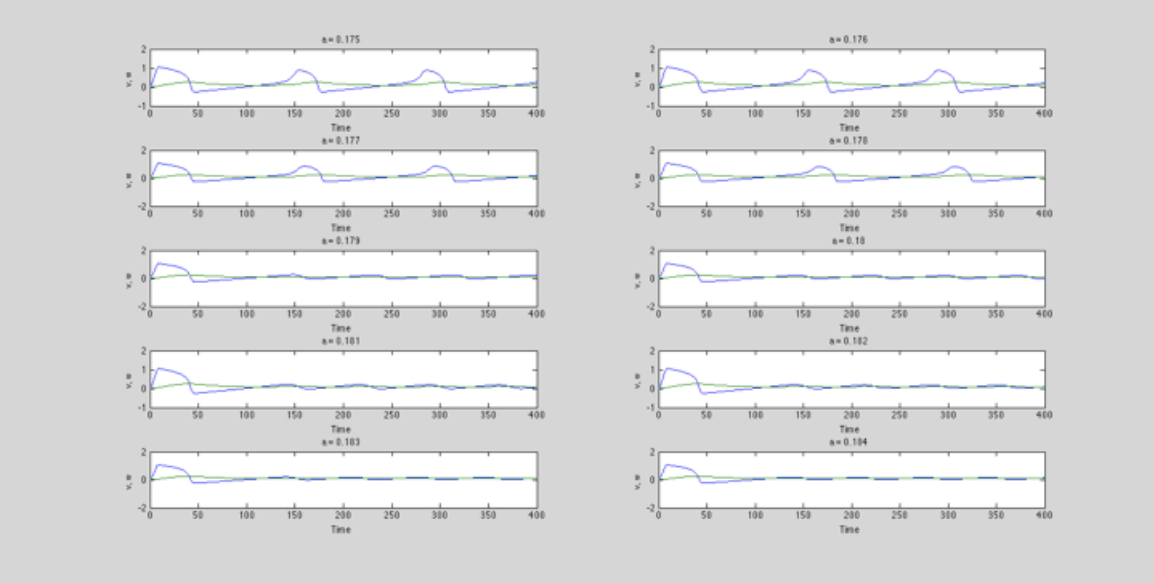

Figure 7b: This figure shows the different simulations of voltage vs. time with the varying parameter, a. A bifurcation occurs when the oscillatory behavior changes to a dampened one.

Although the bifurcations could be visualized with a set of different phase portraits and time courses, we wanted to solve numerically for the eigenvectors as the parameters a, b, and c were varied. The Jacobian used to find these eigenvalues was

$$J = \begin{bmatrix} -3v^2 + (a+2)v - a & -1 \\ b & -c \end{bmatrix}$$

Table 2 below shows these eigenvalues. Notice that the majority of the eigenvalues are complex-valued; thus, some sort of cyclic behavior or spiral is to be expected. It should be noted that only one parameter was varied at a time in order to isolate the effect of that particular parameter. For example, if *a* was varied, all other parameters were held constant.

Varying a,b,c through steps of 0.01										
Value of a (alpha)	0.15	0.16	0.17	0.18	0.19	0.2	0.21	0.22	0.23	0.24
e-value 1	-0.08+0.071414i	-0.085+0.066144i	-0.09+0.06i	-0.095+0.052678i	-0.1+0.043589i	-0.105+0.031225i	-0.11+1.1927e-09i	-0.14702	-0.16583	-0.18179
e-value 2	-0.08-0.071414i	-0.085-0.066144i	-0.09-0.06i	-0.095-0.052678i	-0.1-0.043589i	-0.105-0.031225i	-0.11-1.1927e-09i	-0.082984	-0.074174	-0.068211
Value of b	0.01	0.02	0.03	0.04	0.05	0.06	0.07	0.08	0.09	0.1
e-value 1	-0.08+0.071414i	-0.08+0.12288i	-0.08+0.15843i	-0.08+0.18735i	-0.08+0.21237i	-0.08+0.23473i	-0.08+0.25515i	-0.08+0.27404i	-0.08+0.29172i	-0.08+0.30838i
e-value 2	-0.08-0.071414i	-0.08-0.12288i	-0.08-0.15843i	-0.08-0.18735i	-0.08-0.21237i	-0.08-0.23473i	-0.08-0.25515i	-0.08-0.27404i	-0.08-0.29172i	-0.08-0.30838i
Value of c	0.01	0.02	0.03	0.04	0.05	0.06	0.07	0.08	0.09	0.1
e-value 1	-0.08+0.071414i	-0.085+0.075993i	-0.09+0.08i	-0.095+0.083516i	-0.1+0.086603i	-0.105+0.089303i	-0.11+0.091652i	-0.115+0.093675i	-0.12+0.095394i	-0.125+0.096825i
e-value 2	-0.08-0.071414i	-0.085-0.075993i	-0.09-0.08i	-0.095-0.083516i	-0.1-0.086603i	-0.105-0.089303i	-0.11-0.091652i	-0.115-0.093675i	-0.12-0.095394i	-0.125-0.096825i

Table 2: Sample of varying eigenvalues corresponding to the 3 different figures shown below. Input values as a default were a=0.15, b=0.01, c=0.01 and I0 = 0.1 (input current). The parameters were then varied one at a time.

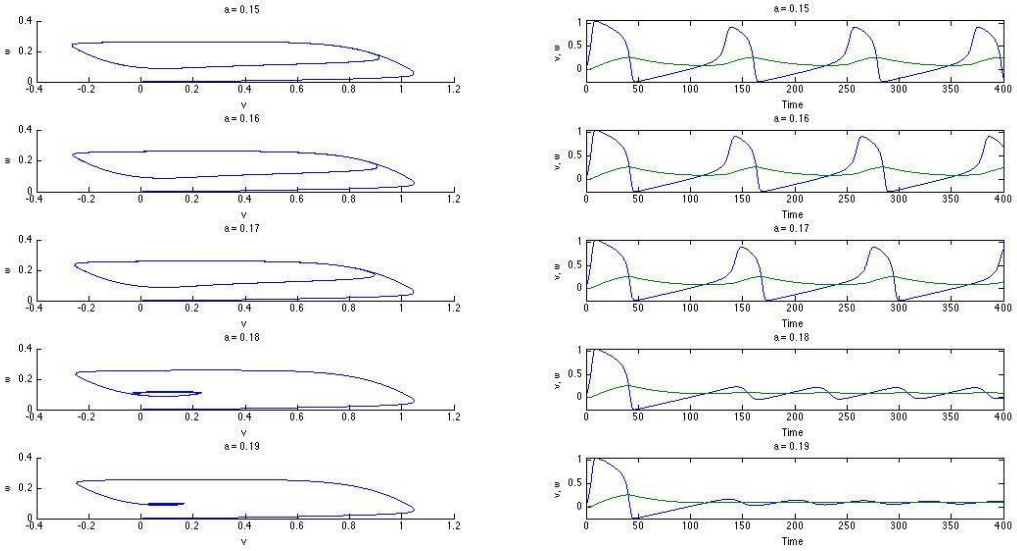

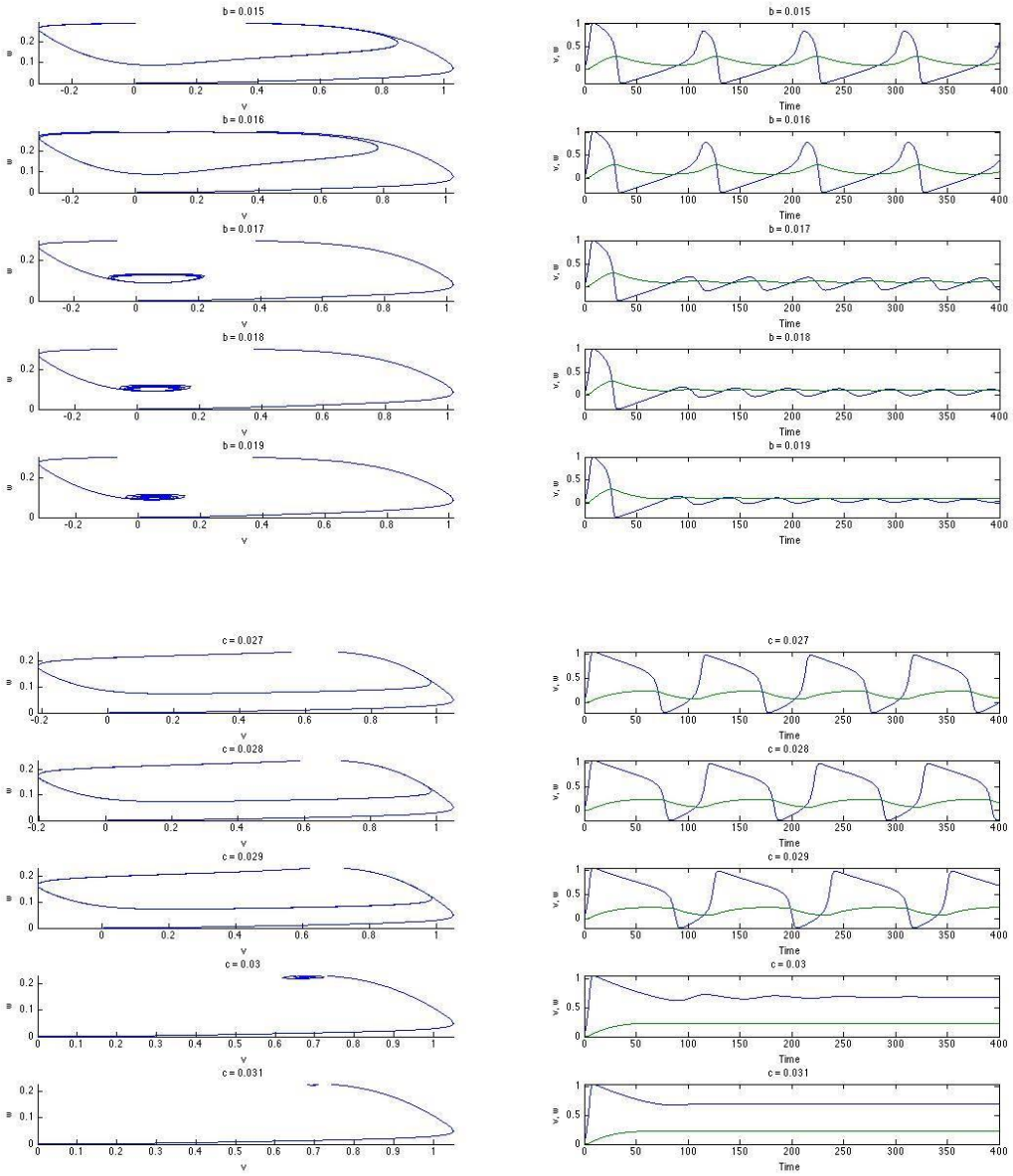

Figures 8, 9, 10: These two rows of figures shows on the left, the phase portrait and the behavior of the dynamical system. The right hand side shows the time courses of v and w. These are corresponding to the 10 different eigenvalues in Table 2. Figure 8 shows the dynamics when parameter a is varied; Figures 9 and 10 show likewise when b and c are varied, respectively.

The above graphs are consistent with what we know about the FHN model. The parameter *a* defines the threshold of excitability; therefore, raising *a* will make it more difficult to elicit sustained oscillations. The phase portrait in Figure 8 confirms this phenomenon, since the limit cycle disappears and υ and ω decay to zero as *a*

increases. The individual decays of υ and ω are evident in their time courses shown in Figure 8.

The ω nullcline is defined by ω = b/c*υ; therefore, changing *b* and *c* will change the slope of the line. An increase in *b* corresponds to a steeper slope. As graphically visualized in Figure 6, this will cause the w-nullcline to intersect the υ-nullcline eventually in one location instead of three. Thus, as *b* increases, the number of fixed points decreases. This is confirmed in Figure 9 by the disappearance of the limit cycle and the decay of the υ and ω time courses to 0.

Increasing *c* has the opposite effect of *b*, as *c* decrease the slope of the ω-nullcline. Graphically, this can be seen in Figure 6; as the ω-nullcline flattens out, more intersections between the υ- and ω-nullclines become possible. Thus, the number of fixed points increases from 1 to 3. Similar to parameters *a* and *b,* this phenomenon is confirmed in the phase portraits and time courses in Figure 10. Specifically, a limit cycle appears at the critical value of *c* (the c bifurcation point) and sustained oscillations of υ become possible.

Clinical Application of Neuronal Modeling

Epilepsy is a neurological disorder which is characterized by seizures and it affects 65 million people worldwide[8]. Mechanistically, the neurons fire non-synchronously which causes temporary cognitive impairment and loss of motor coordination. This is due to excessive excitatory response due to a mutation in the potassium ion channel in the central nervous system (CNS)[7]. The potassium channel has a loss of functionality which induces it to lose conductivity as defined by the neuron model. The following figure showcases the result of losing potassium ion channel conductivity. As a continuous current is applied, the membrane potential of the neuron does not return to resting potential, due to the lack of potassium out-flux[7].

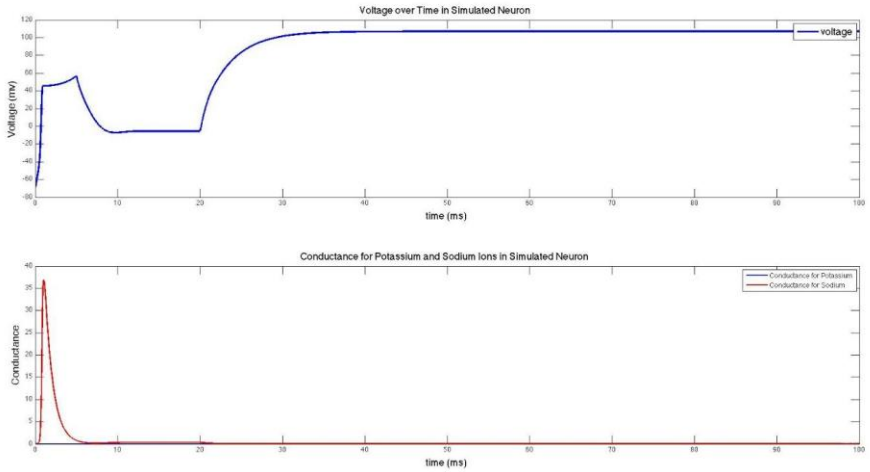

Figure 11: The loss of functionality of the the potassium ion channel causes the neuron to not recover the electrochemical potential. Therefore in application of a continuous current, a constant depolarization is seen.

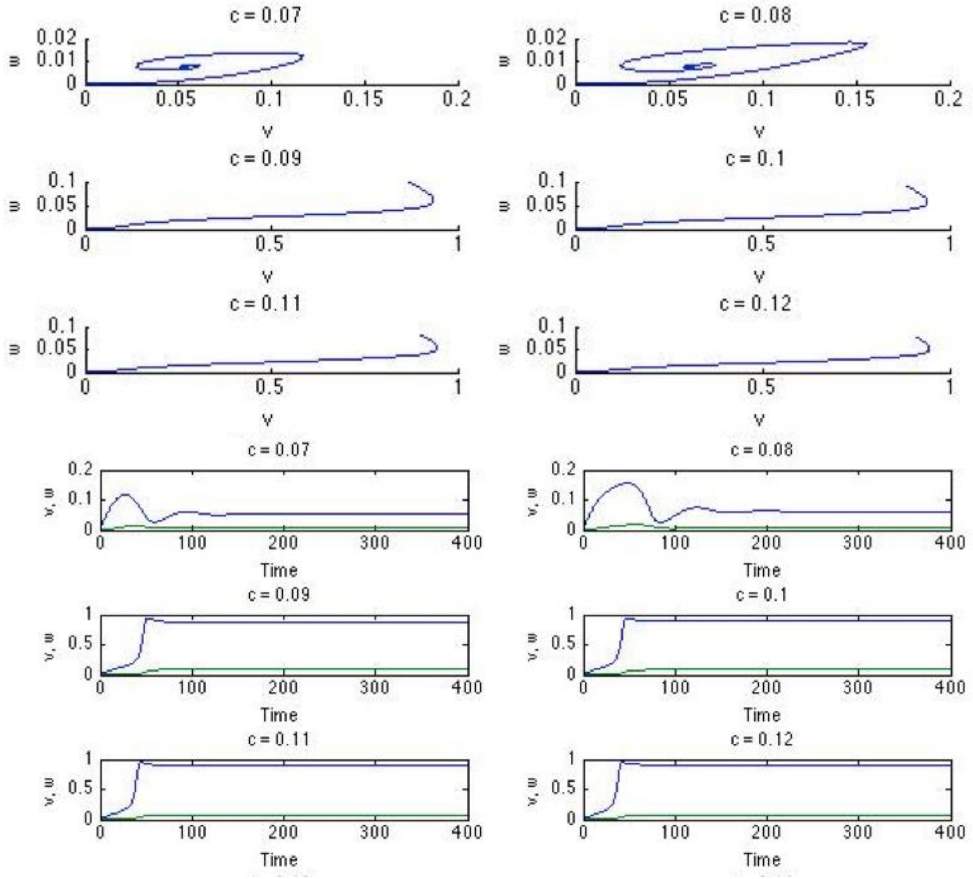

Figure 12a,b: Varying the parameter 'c' in order to change the ion channel recovery kinetics. The limit cycle and stable oscillations disappear when recovery is slowed. As the parameter 'c' increases, the overall kinetics of the membrane potential is slowed.

Therefore, the potassium ion channel cannot respond quickly enough to repolarize the membrane. As seen in Figure 12a, the increasing 'c' parameter makes the limit cycle disappear, indicating that the oscillatory motion of the action potential is no longer occurring. This is relevant to the physiological phenomenon of epilepsy during a seizure, a steady and stable limit cycle is nonexistent. Figure 12b show the time course as a function of 'c'. As 'c' increases, the oscillatory motion decreases and hyper-excitability is induced.

However, there are inherent limitations in utilizing the FitzHugh-Nagumo model for this purpose as all the kinetic recovery variables associated with all ion channels are

grouped in one variable, ‘ω’. Therefore, it is difficult to isolate the functionality of solely the potassium channel.

In addition, because there is a lack of recovery in the system, the model would lose the stable fixed point at the resting potential. In addition, the stable limit cycle that appears after the current reaches a certain threshold for action potential is now nonexistent.

Conclusion

There are inherent tradeoffs when analyzing multi-dimensional nonlinear systems. High order systems, such as the Hodgkin-Huxley model, approximate neuronal firing more accurately, yet are difficult to understand from a qualitative standpoint. However, lower order systems, such as the FitzHugh-Nagumo Model, are easier to interpret qualitatively, yet can lack precision needed when manipulating specific parameters, such as potassium channels for epilepsy. Most likely, a combination of models will have to be used to understand the neuronal dynamics and to find the balance between accuracy and feasibility.

References

1. Hoff, Robert D. "Qualcomm's Neuromorphic Chips Could Make Robots and Phones More Astute About the World | MIT Technology Review." *MIT Technology Review*. N.p., n.d. Web. 12 June 2014.
2. Hodgkin, A. L., and A. F. Huxley. "A Quantitative Description of Membrane Current and Its Application to Conduction And Excitation In Nerve." *Journal of Physiology* 117 (1952): 500-44. *PubMed*. Web.
3. Izhikevich, Eugene M. *Dynamical Systems in Neuroscience: The Geometry of Excitability and Bursting*. Cambridge, MA: MIT, 2007. Print.
4. Strogatz, Steven Henry. *Nonlinear Dynamics and Chaos: With Application to Physics, Biology, Chemistry, and Engineering*. Cambridge: Westview, 2000. Print.
5. Izhikevich, Eugene M., and Richard FitzHugh. "FitzHugh-Nagumo Model."*Scholarpedia*. Scholarpedia, 2006. Web.
6. Hubner, Christian A., and Thomas J. Jentsch. "Human Molecular Genetics."*Ion Channel Diseases*. Oxford Journals, 4 July 2002. Web. <http://hmg.oxfordjournals.org/content/11/20/2435.full#sec-7>
7. Lerche, H., K. Jurkat-Rott, and F. Lehmann-Horn. "Ion Channels and Epilepsy."*American Journal of Medical Genetics* 2nd ser. 106 (2011): 146-59. *PubMed*. Web.
8. Thurman, DJ; Beghi, E; Begley, CE; Berg, AT; Buchhalter, JR; Ding, D; Hesdorffer, DC; Hauser, WA; Kazis, L; Kobau, R; Kroner, B; Labiner, D; Liow, K; Logroscino, G; Medina, MT; Newton, CR; Parko, K; Paschal, A; Preux, PM; Sander, JW; Selassie, A; Theodore, W; Tomson, T; Wiebe, S; ILAE Commission on, Epidemiology (September 2011). "Standards for epidemiologic studies and surveillance of epilepsy.". *Epilepsia*. 52 Suppl 7: 2–26.